Journal of Physiology (1991), **434**, *pp.* 609–626
With 8 figures
Printed in Great Britain

POST-INHIBITORY EXCITATION AND INHIBITION IN LAYER V PYRAMIDAL NEURONES FROM CAT SENSORIMOTOR CORTEX

BY W. J. SPAIN, P. C. SCHWINDT AND W. E. CRILL

From the Department of Physiology & Biophysics and Department of Medicine (Division of Neurology), University of Washington School of Medicine, Seattle, WA 98195, USA

(*Received 19 January 1990*)

SUMMARY

1. The effect of conditioning pre-pulses on repetitive firing evoked by intracellular current injection was studied in layer V pyramidal neurones in a brain slice preparation of cat sensorimotor cortex. Most cells displayed spike frequency adaptation (monotonic decline of firing rate to a tonic value) for several hundred milliseconds when depolarized from resting potential, but the cells differed in their response when pre-pulses to other potentials were employed. In one group of cells, the initial firing rate increased as the pre-pulse potential was made more negative (post-hyperpolarization excitation). Adaptation was abolished by depolarizing pre-pulses. In a second group, the initial firing rate decreased as the pre-pulse potential was made more negative (post-hyperpolarization inhibition). Hyperpolarizing pre-pulses caused the initial firing to fall below and accelerate to the tonic rate over a period of several seconds. A third group displayed a mixture of these two responses: the first three to seven interspike intervals became progressively shorter and subsequent intervals became progressively longer as the conditioning pre-pulse was made more negative (post-hyperpolarization mixed response).

2. Cells were filled with horseradish peroxidase or biocytin after the effect of pre-pulses was determined. All cells whose firing patterns were altered by pre-pulses were large layer V pyramidal neurones. Cells showing post-hyperpolarization excitation or a mixed response had tap root dendrites, fewer spines on the apical dendrite and larger soma diameters than cells showing post-hyperpolarization inhibition.

3. Other electrophysiological parameters varied systematically with the response to conditioning pre-pulses. Both the mean action potential duration and the input resistance of cells showing post-hyperpolarization excitation were about half the values measured in cells showing post-hyperpolarization inhibition. Values were intermediate in cells showing a post-hyperpolarization mixed response. The after-hyperpolarization following a single evoked action potential was 20 % briefer in cells showing post-hyperpolarization excitation compared to those showing inhibition.

4. Membrane current measured during voltage clamp suggested that two ionic mechanisms accounted for the three response patterns. Post-hyperpolarization excitation was caused by deactivation of the inward rectifier current (I_h). Selective reduction of I_h with extracellular caesium diminished post-hyperpolarization ex-

citation, whereas blockade of calcium influx had no effect. Post-hyperpolarization inhibition was caused by enhanced activation of a slowly inactivating potassium current. Selective reduction of this current with 4-aminopyridine diminished the post-hyperpolarization inhibition.

5. Chord conductances underlying both I_h and the slow-transient potassium current were measured and divided by leakage conductance to control for differences in cell size. The normalized G_h was larger in cells showing post-hyperpolarization excitation or a mixed response than in those showing post-hyperpolarization inhibition. No consistent difference in the normalized slow-transient potassium conductance was found among cells, but its decay time course was more rapid in cells showing post-hyperpolarization inhibition.

6. We conclude that cat sensorimotor cortex contains at least three functional groups of large layer V pyramidal cells as distinguished by the effects of subthreshold pre-pulses on repetitive firing patterns. The characteristic effect of pre-pulses in each group is determined by different expression of the channels underlying the inward rectifier current and the slow-transient potassium current.

INTRODUCTION

Impulse activity in primate corticospinal neurones during trained behavioural tasks correlates with various parameters of movement and force (Evarts, 1968; Cheney & Fetz, 1980). Recently, Lemon & Mantel (1989) found that relatively small changes in the instantaneous discharge frequency of individual corticomotoneuronal neurones influenced the magnitude and modulation of electromyogram (EMG) activity in the monkey. These experiments demonstrate that the discharge patterns of single central neurones have physiological significance, and provide the rationale for experiments designed to identify the rules for transducing synaptic input into spike trains.

Variations in firing patterns among pyramidal neurones can result both from differences in the synaptic currents driving the neurones and from differences in their intrinsic membrane properties. Neurones have a great diversity of channel types which control their repetitive firing properties. Many of these ionic conductance mechanisms have strong voltage dependence and slow kinetics in the subthreshold range of membrane potential (Llinás, 1988). Consequently, the value of the interspike membrane potential can affect subsequent impulse patterns. For example, several ionic conductances have a voltage-dependent inactivation that is removed by membrane hyperpolarization. Inferior olivary and thalamic neurones have a large subthreshold transient calcium conductance that markedly alters the pattern of neurone firing following membrane hyperpolarization (Llinás & Yarom, 1981; Llinás & Jahnsen, 1982). Connor & Stevens (1971) showed that membrane hyperpolarization removes inactivation of a transient potassium current (I_A) and subsequent excitation is delayed by activation of I_A. This latter mechanism for transiently changing repetitive firing properties has been demonstrated in a number of mammalian central neurones (Segal, 1985; Dekin, Getting & Johnson, 1987; Storm, 1988; Bargas, Galarraga & Aceves, 1989).

Here we examine the effects of conditioning membrane polarization upon the repetitive firing evoked by a test current pulse in layer V pyramidal neurones in cat.

Three distinct response patterns associated with differences in cellular structure and other physiological properties are identified. Evidence is presented for the ionic mechanisms underlying these dissimilar responses.

METHODS

All experimental procedures were identical to those in the previous paper (Spain, Schwindt & Crill, 1991). Most data were obtained from a different set of recorded neurones. One additional extracellular solution was used containing 2 or 3 mM-CsCl substituted equimolar for NaCl.

For intracellular staining, the recording electrodes were filled with either horseradish peroxidase (HRP) solution (Boehringer, 5 mg in 50 μl of 0·5 M-KCl and 0·05 M-Tris (pH = 8)) or 2% biocytin in 1 M-KCl. For all other physiological studies the electrodes were filled with 3 M-KCl. DC resistances of the HRP-filled electrodes were 9–53 MΩ. Biocytin-filled electrodes were 8–30 MΩ. KCl electrodes were 7–15 MΩ. Intracellular neuronal staining using either HRP or biocytin was achieved by passing depolarizing current pulses (1–6 nA) at 2 Hz (80% duty cycle) for 10–30 min. Slices with stained neurones were maintained in the recording chamber for about 1 h to allow HRP or biocytin to diffuse throughout the neurone. The tissue was subsequently fixed in 4% paraformaldehyde and 1·25% gluteraldehyde in phosphate-buffered saline (HRP) or 10% neutral-buffered formalin (biocytin) for 2 h and left overnight in 0·1 M-phosphate buffer solution containing 20% sucrose. Frozen slices were sectioned at 80 μm intervals. Sections for HRP processing were rinsed in a 0·1 M-phosphate buffer, reacted by the cobalt-enhanced diaminobenzidine (DAB) method (Adams, 1981), mounted on glass slides and counter-stained with Cresyl Violet. Sections for biocytin processing were rinsed in a 0·1 M-phosphate-buffered saline (PBS) followed by incubation at room temperature for 2 h, according to the manufacturer's directions, in streptavidin–biotin–HRP complex (Zymed) and 0·1% Triton-X (Horikawa & Armstrong, 1988). Cells in PBS-rinsed slices were subsequently visualized by the cobalt-enhanced DAB reaction.

Graphs were made of the instantaneous firing frequency evoked by constant injected current pulses *versus* time by plotting the reciprocal of each interspike interval at the time of occurrence of the second action potential in that interspike interval. The points in these plots are connected only for clarity.

RESULTS

Eighty-seven neurones from area 4γ of the sensorimotor cortex from twenty cats were studied. Resting potential was -67 ± 4 mV (mean $\pm$ S.D.), and there was no spontaneous firing. Action potential height was 93 ± 9 mV. Repetitive firing was evoked by injection of a test current pulse through the recording microelectrode. All neurones showed repetitive firing in response to steady injected current pulses. Tonic firing rate increased monotonically with current strength (Stafstrom, Schwindt & Crill, 1984).

Effects of subthreshold membrane potential changes on subsequent firing patterns

When depolarized from resting potential, most cells exhibited spike frequency adaptation consisting of a decline in firing rate over several hundred milliseconds from a fast initial rate to a slower tonic rate (Stafstrom *et al.* 1984). In the majority of impaled neurones, the initial firing rate was markedly altered and the pattern of firing was changed when conditioning pre-pulses ranging from -60 to -100 mV preceded the test depolarization. The effects of these pre-pulses were most prominent when the tonic firing was < 50 Hz; therefore, the test current pulses were adjusted accordingly to keep firing rate low. In thirteen of the eighty-seven cells, the initial firing rate evoked by the test current pulse became faster as pre-pulses were made more negative: this is termed post-hyperpolarization excitation. In fifty-five other

cells the initial rate became slower as pre-pulses were made more negative (post-hyperpolarization inhibition). In twelve other neurones early interspike intervals shortened but later intervals lengthened as pre-pulses were made more negative (post-hyperpolarization mixed response). The repetitive firing of seven cells was not altered significantly by conditioning pre-pulses.

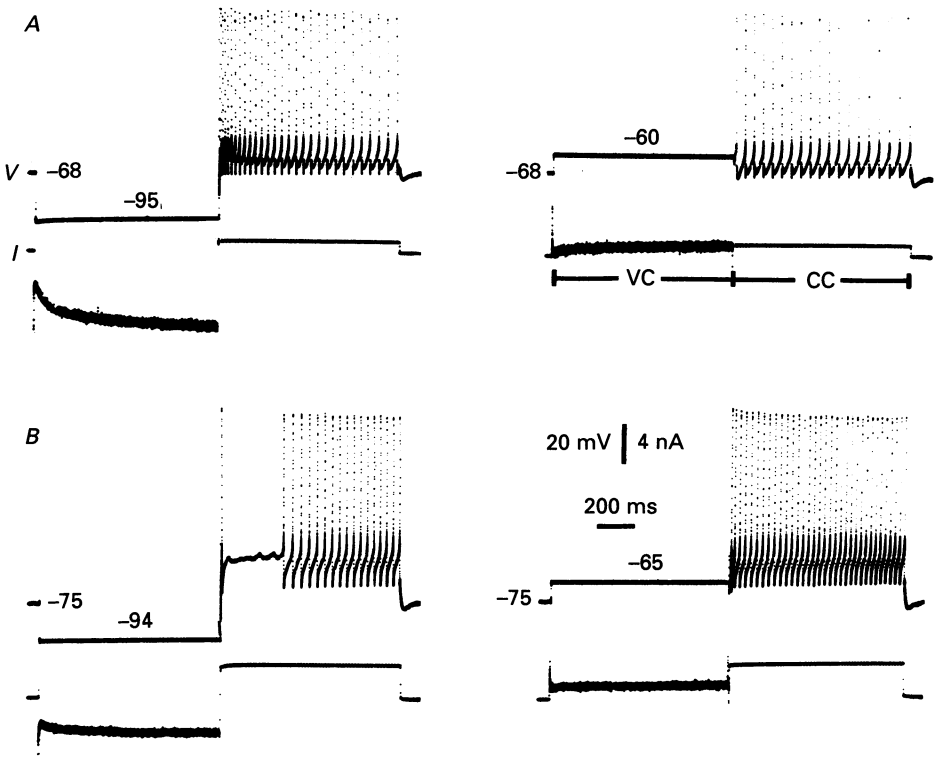

Fig. 1. Cells showing post-hyperpolarization excitation and post-hyperpolarization inhibition. *A*, repetitive firing evoked by an injected constant current pulse in a cell showing post-hyperpolarization excitation: initial firing rate is faster after a hyperpolarizing pre-pulse (left panel) than depolarizing pre-pulse (right panel). Resting potential −68 mV. *B*, a different cell showing post-hyperpolarization inhibition: initial firing rate is slower after a hyperpolarizing pre-pulse (left panel) than a depolarizing pre-pulse (right panel). Resting potential −75 mV. Calibration bars apply to all panels. VC, single-electrode voltage clamp; CC, constant current stimulation.

Post-hyperpolarization excitation

Figure 1*A* shows the experimental protocol. Single-microelectrode voltage clamp was used to keep the membrane potential constant during the pre-pulse (VC in Fig. 1*A*, right); the recording mode was then suddenly switched to constant current stimulation to evoke repetitive firing (CC in Fig. 1*A*, right). The magnitude of the test injected current pulse was kept constant in each trial while the conditioning pre-pulse voltage was varied.

The cell of Fig. 1*A* showed post-hyperpolarization excitation. Initial firing rate

after the 1 s pre-pulse to −95 mV (Fig. 1*A*, left) was faster than after the pre-pulse to −60 mV (Fig. 1*A*, right). The plots of instantaneous firing rate *vs.* time in Fig. 2*A*, left, show how peak firing rate became faster as 1 s pre-pulses were made more negative. Notice that purely tonic firing (no adaptation) followed the pre-pulse to

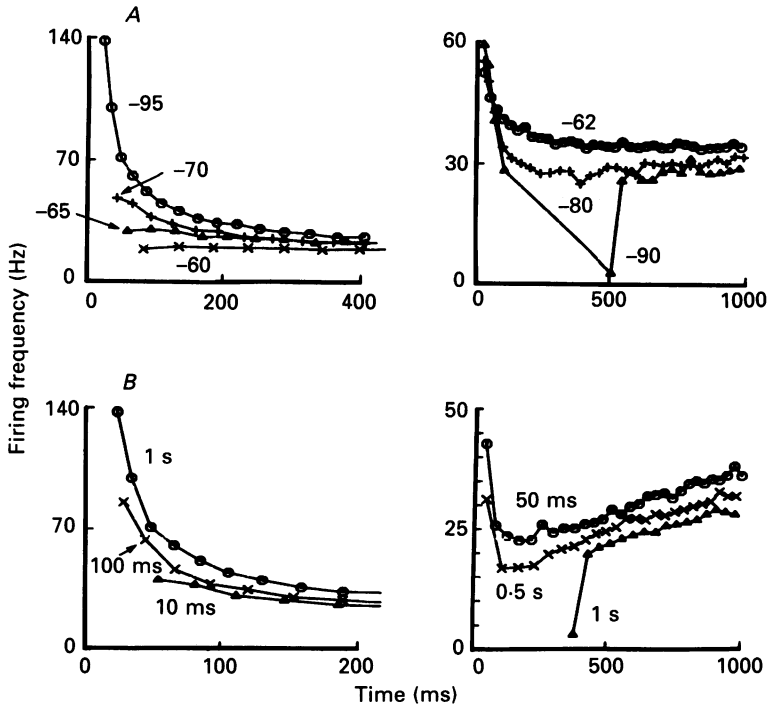

Fig. 2. Alteration of firing rate by pre-pulses is graded with voltage and time. *A*, instantaneous firing rate *versus* time after terminating a 1 s pre-pulse to the potentials indicated (mV). Left, cell showing post-hyperpolarization excitation. Right, cell showing post-hyperpolarization inhibition. *B*, instantaneous firing rate *versus* time for different duration pre-pulses to −95 mV. Left, cell showing excitation (same as in *A*). Right, cell showing inhibition. Test current pulses were 1 nA (*A*, left; *B*, left), 2 nA (*A*, right) and 3 nA (*B*, right).

−60 mV. Changing the pre-pulse potential to −70 mV caused peak firing rate to increase threefold above the tonic rate; changing the pre-pulse to −95 mV caused a sevenfold increase. No further increase in peak firing rate followed pre-pulses more negative than −100 mV.

In thirteen cells, hyperpolarizations from resting potential of 1 s duration and 20 mV amplitude increased peak firing rate by 120% on average (range: 50–280%) compared to the response evoked from resting potential. The rate increase lasted for 200–800 ms. The increase in firing rate depended upon pre-pulse duration (Fig. 2*B*, left). At least 90% of the increase in peak rate produced by a given pre-pulse occurred with pre-pulse durations of 1 s (durations up to 8 s were tested).

Post-hyperpolarization inhibition

The cell of Fig. 1*B* showed post-hyperpolarization inhibition. Firing rate slowed and firing paused for several hundred milliseconds as the pre-pulse potential was made more negative. This slowing or pause of firing usually occurred after one or two

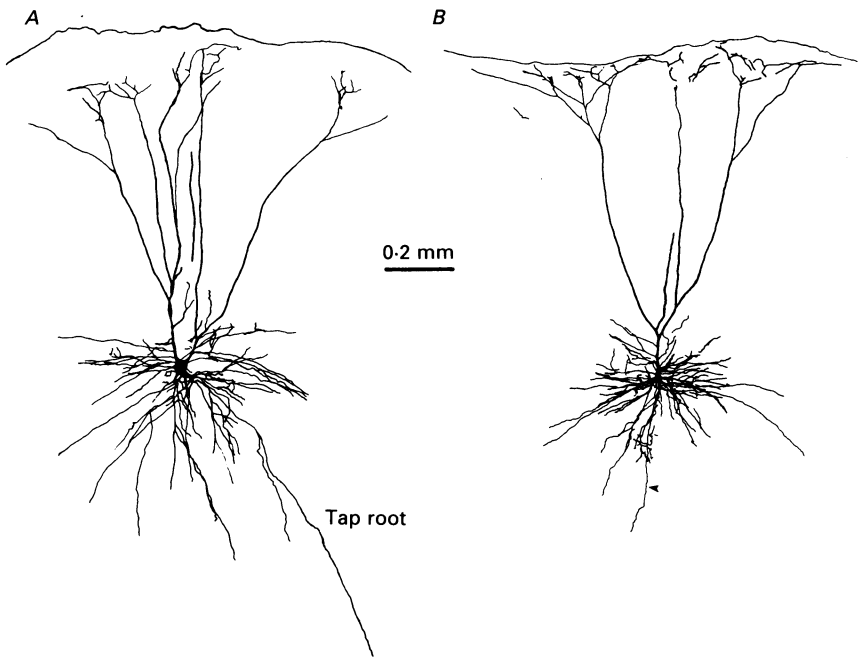

Fig. 3. Camera lucida reconstructions of two cells filled with biocytin. The topmost line of each drawing represents the pia. Both somas were in layer V. The arrow-head in *B* points to the axon. The axon could not be identified in *A*. Note the prominent oblique tap root dendrite in *A*. The same scale bar applies to both cells. Cell in *A* showed post-hyperpolarization excitation (input resistance was 8 MΩ) and cell in *B* showed post-hyperpolarization inhibition (input resistance was 21 MΩ).

initial spikes. The post-hyperpolarization inhibition was graded with pre-pulse potential and duration (Fig. 2, right panels). In the fifty-five cells showing this response, firing rate decreased by $\geqslant 15\%$ following 20 mV, 1 s hyperpolarizations compared to the response evoked by depolarization from resting potential. The maximal decrease in firing rate occurred 50–400 ms after the start of the firing; firing rate subsequently accelerated to the tonic rate over a period of 800 ms–5 s.

Post-hyperpolarization mixed response

Twelve neurones responded to hyperpolarizing pre-pulses with an early increase and a late decrease of firing rate compared to responses evoked from resting potential. The plot of Fig. 5*D* shows how the firing pattern was altered by a hyperpolarizing pre-pulse in a mixed response cell. In these cells, the increase in firing rate occurred during the first three to seven interspike intervals (lasting 60–200 ms).

Hyperpolarizations of 1 s duration and 20 mV amplitude increased peak firing rate by 90% (range: 20–270%) and decreased the late firing rate by an average of 12% compared to responses evoked by depolarization from resting potential.

All three groups of cells are layer V pyramidal neurones

Neurones were filled with horseradish peroxidase (HRP) or biocytin (see Methods) after determining the effect of pre-pulses on firing patterns. Camera lucida reconstructions of two typical cells are shown in Fig. 3. Both were large layer V pyramidal neurones, though one showed excitation and the other inhibition following the hyperpolarizing pre-pulse. Nineteen filled neurones were recovered after physiological characterization. Seventeen of these cells were large layer V pyramidal neurones and included two cells that showed excitation, nine that showed inhibition and six showed that a mixed response to prior hyperpolarization. The repetitive firing pattern of the remaining two cells were not affected by conditioning hyperpolarization; they appeared to be pyramidal neurones, but were much smaller than the other seventeen cells. One of these neurones was located in the middle of layer III, and the other was at the boundary of layer V and VI.

Cells showing either post-hyperpolarization excitation or a mixed response had fewer spines on their main apical dendrites and larger somata (diameter = 29 ± 5 μm, mean $\pm$ S.D., $n = 8$) than those cells showing inhibition (16 ± 3 μm, $n = 9$). Prominent oblique tap root dendrites which are typical of fast-conducting corticofugal neurones (Samejima, Yamamato, Ito & Oka, 1985) were present only on the cells showing excitation ($n = 1$) or a mixed response ($n = 4$).

Action potential duration and input resistance varied with response type

Action potential durations were longest in cells showing post-hyperpolarization inhibition, shortest in cells showing post-hyperpolarization excitation and intermediate in cells showing a mixed response (Fig. 4; Table 1). These differences between each group of neurones were statistically significant (two-tailed t test, $P < 0{\cdot}01$). As shown in Fig. 4*A* and *B*, the duration of the after-hyperpolarization following a single evoked action potential was significantly shorter in cells showing post-hyperpolarization excitation than those showing post-hyperpolarization inhibition ($P < 0{\cdot}01$; see also Table 1).

Input resistance, as computed from the maximal voltage response evoked by a $-0{\cdot}5$ nA current pulse, also varied systematically with response type. It was highest in cells showing post-hyperpolarization inhibition, intermediate in those showing a mixed response and lowest in those showing post-hyperpolarization excitation. These results are summarized in the histogram of Fig. 4*D* and in Table 1. The differences between each group of cells were statistically significant (two-tailed t test, $P < 0{\cdot}01$). The low input resistance of cells showing post-hyperpolarization excitation was probably not caused by impalement injury because their action potentials had the shortest durations, and their resting potentials were similar to the other two groups (Table 1).

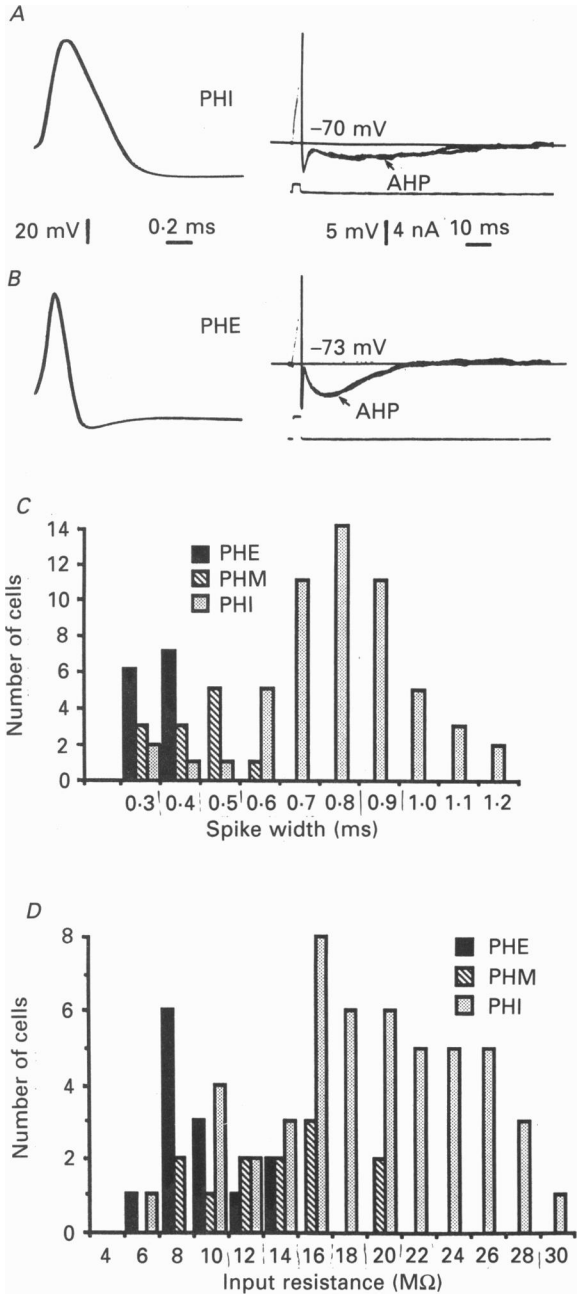

Fig. 4. Action potential duration and input resistance vary with response type. *A*, a cell showing post-hyperpolarization inhibition. Left, action potentials evoked by 3 ms current pulses. Right, same data at slower recording speed. *B*, a cell showing post-hyperpolarization excitation. Left, action potentials evoked by a 3 ms current pulse. Right, same data at slower recording speed. Resting potential of each cell is indicated by continuous horizontal lines. AHP, after-hyperpolarization. Calibration bars apply to *A* and *B*. Action potentials retouched. *C*, distribution of action potential durations for cells

Ionic mechanisms underlying the alteration of firing rate by pre-pulses

Single-microelectrode voltage clamp was used to examine ionic currents following conditioning pre-pulses. The effect of pre-pulses on a cell's firing pattern was first observed, and the perfusing solution was then changed to one containing TTX (1 μM) and cadmium (400 μM), or TTX, 5 mM-$MgCl_2$, 0·5 mM-EGTA and no added calcium.

TABLE 1. Properties of neurones by cell type

Property	PHE	PHI	PHM
Resting potential (mV)	$-69 \pm 2{\cdot}9$ (13)	-67 ± 4 (55)	-67 ± 4 (12)
Action potential height (mV)	88 ± 8 (13)	96 ± 8 (55)	85 ± 7 (12)
Action potential duration* (ms)	$0{\cdot}36 \pm 0{\cdot}05$ (13)	$0{\cdot}80 \pm 0{\cdot}19$ (55)	$0{\cdot}46 \pm 0{\cdot}09$ (12)
Input resistance† (MΩ)	9 ± 3 (13)	21 ± 8 (55)	14 ± 4 (12)
AHP duration (ms)	39 ± 7 (7)	54 ± 13 (29)	48 ± 8 (12)

* Measured at action potential threshold.
† Computed from the maximal voltage response to −0·5 nA current pulses.
Values are given as means ± S.D. followed by the number n in parentheses.

Figure 5 shows membrane currents evoked by a test voltage step with and without a preceding hyperpolarizing pre-pulse. There was good correlation between the observations in current clamp and voltage clamp: if the hyperpolarizing pre-pulse caused excitation in current clamp, it resulted in a more inward early current during voltage clamp (Fig. 5*A*), whereas cells that were inhibited showed a more outward current (Fig. 5*B*). Cells showing a mixed response in current clamp (Fig. 5*D*) showed a combination of effects in voltage clamp, a more inward early current and a more outward late current (Fig. 5*C*). We postulated that the faster firing rate and more inward current following hyperpolarization were caused by deactivation of the hyperpolarization-activated cation current, I_h (see Spain, Schwindt, & Crill, 1987), whereas the slowing of firing rate and more outward current were caused by removal of inactivation of the slow-transient potassium current (see Spain *et al.* 1991). These hypotheses were tested by selective pharmacological reduction of I_h and the slow-transient potassium current as described below.

Role of I_h

I_h activates at potentials negative to −55 mV; it is reduced by extracellular caesium in a voltage-dependent manner such that the block begins at −65 mV and becomes more effective upon hyperpolarization (Spain *et al.* 1987). Figure 6*A* and *B*

of the three classes (post-hyperpolarization excitation, PHE; post-hyperpolarization inhibition, PHI; and post-hyperpolarization mixed response, PHM). Action potential durations were measured at threshold. Histogram bin width: 0·1 ms. *D*, distribution of input resistance among cells of the same groups. Six PHI cells with input resistance of 32–40 MΩ are not shown. Histogram bin width: 2 MΩ.

shows this voltage-dependent reduction of I_h as measured during application of hyperpolarizing pre-pulses to a cell showing post-hyperpolarization excitation. The dashed line in Fig. 6*B* indicates that hyperpolarization to −90 mV in caesium was required to evoke the same I_h as a step to −80 mV did in normal perfusate. I_h at

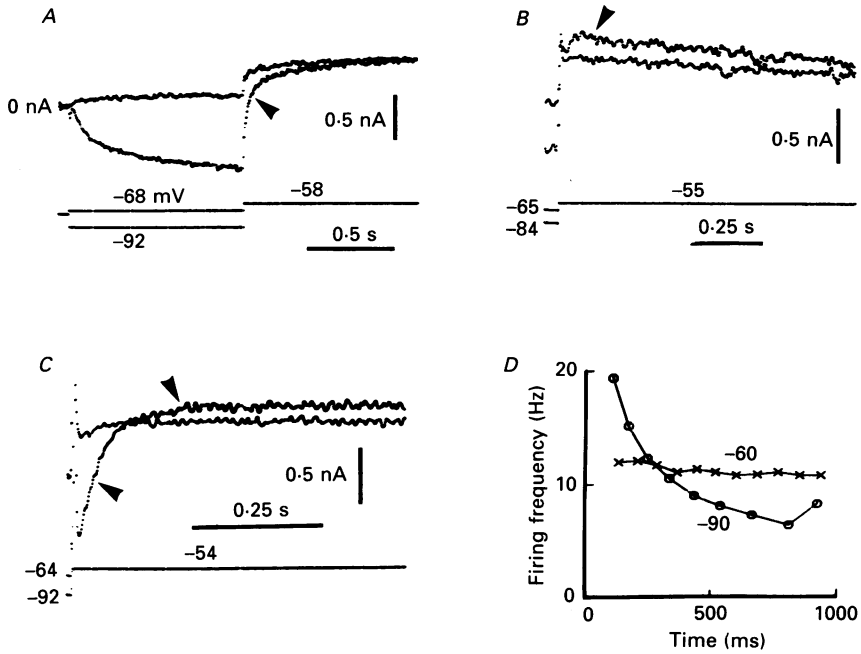

Fig. 5. Effect of conditioning pre-pulses on ionic currents. Voltage-clamp records from three cells that showed post-hyperpolarization excitation (*A*), inhibition (*B*) and mixed response (*C*) following a hyperpolarizing pre-pulse. TTX and cadmium present. Membrane potential is shown in lower traces. The upper traces show currents. The current trace marked with an arrow-head was evoked following the more negative of the two pre-pulses. In *B* and *C*, the pre-pulses are not shown in full. Leakage current was subtracted from total current records in *A* and *B*. *D*, instantaneous firing rate *versus* time following 1 s pre-pulses to the potentials indicated (mV) from the cell of *C* prior to the addition of TTX and cadmium to the solution. Test current pulse was 1·2 nA.

−60 mV was not altered by caesium. Figure 6*C* and *D* shows that caesium reduced peak firing rates obtained after all pre-pulses negative to −60 mV. The peak firing rate after a pre-pulse to −90 mV in caesium (60 Hz) was the same as after a pre-pulse to −80 mV in normal perfusate. The response following a pre-pulse to −60 mV was unchanged. Thus, there were quantitatively similar effects of caesium on both I_h and firing rates. Similar results were obtained in three other cells.

Evidence of a low-threshold calcium current has been obtained in guinea-pig and rat neocortical neurones (Friedman & Gutnick, 1987; Sutor & Zieglgänsberger, 1987). Removal of inactivation from this current by a hyperpolarizing pre-pulse could contribute to the excitation at the end of the pulse, but it is unlikely that a low-threshold calcium current plays a significant role in the responses described here. In three cells, post-hyperpolarization excitation was not changed by

EGTA-containing, calcium-free solution after calcium-dependent after-hyperpolarizations were blocked.

I_h was consistently larger in cells showing post-hyperpolarization excitation and the mixed response cells than in cells showing post-hyperpolarization inhibition; but

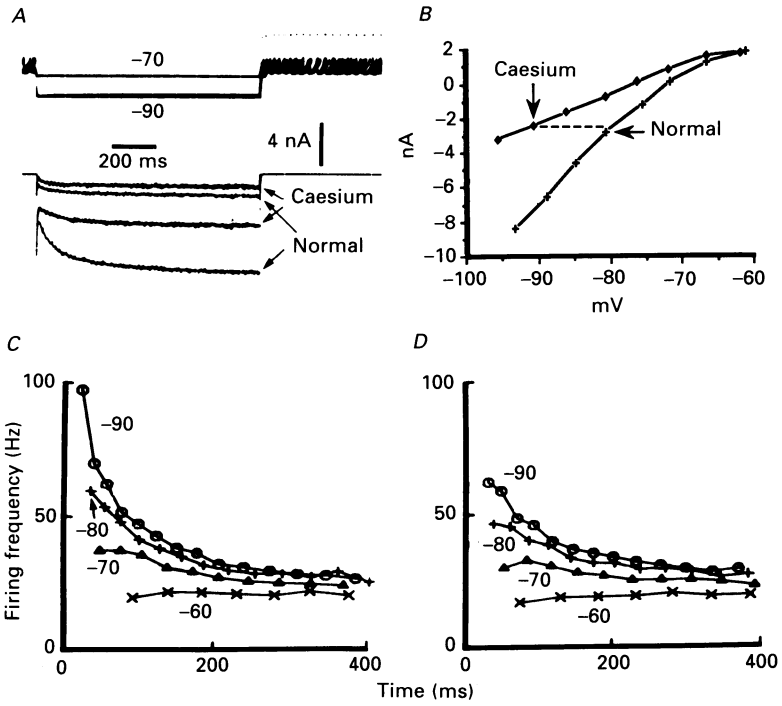

Fig. 6. Reduction of I_h by caesium reduces post-hyperpolarization excitation. All records from the same cell. *A*, hyperpolarizing voltage steps to −70 and −90 mV in normal perfusate (labelled normal) and after addition of 2 mM-CsCl to the bath (labelled caesium). These steps served as pre-pulses for repetitive firing evoked by tonic current injection (2·5 nA). *B*, current–voltage relation measured at the end of 1 s hyperpolarizing voltage steps (as in *A*) before and after caesium application. *C* and *D*, plots of instantaneous firing frequency *versus* time following 1 s pre-pulses to the four indicated potentials in normal perfusate (*C*) and after the addition of caesium (*D*).

this difference could reflect the difference in surface area. We used leakage conductance measured at resting potentials as an index of cell size as described in the preceding paper (Spain *et al.* 1991). The chord conductance (G_h) was calculated from I_h measured at ≈ -84 mV (near half-activation) using an estimated reversal potential of −45 mV. G_h was then normalized by dividing by the leakage conductance. Cells showing post-hyperpolarization excitation ($n = 10$) and the mixed response ($n = 5$) had a larger normalized G_h (0·58 ± 0·65, mean ± S.D.) than cells showing post-hyperpolarization inhibition (0·30 ± 0·16, $n = 24$). These differences were statistically significant (two-tailed t test; $P < 0·05$). Figure 8*A* shows the distribution of normalized G_h for these two populations of neurones. G_h is

partially active at resting potential and contributes to the apparent leakage conductance (Spain *et al.* 1987), but this would tend to decrease differences in the normalized G_h.

Role of slow-transient potassium current

Low doses of 4-aminopyridine selectively reduce the slow-transient potassium current (Spain *et al.* 1991). The possible role of this current in post-hyperpolarization

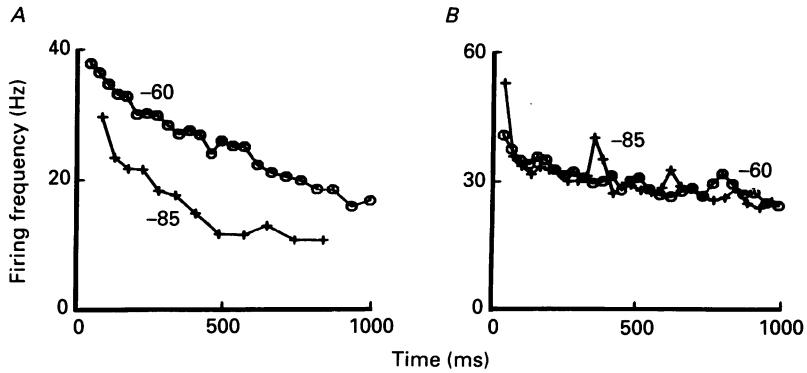

Fig. 7. Reduction of the slow-transient potassium current by 4-aminopyridine abolishes post-hyperpolarization inhibition. Plots of instantaneous firing rate *versus* time following 1 s conditioning pre-pulses to the potentials indicated (mV) before (*A*) and after (*B*) addition of 600 μM-4-aminopyridine to the bath. Cadmium (400 μM) was present in *A* and *B*. Test current pulse was 0·5 nA.

inhibition was tested by measuring the effect of pre-pulses on firing before and after application of 4-aminopyridine as shown in Fig. 7. In this cell post-hyperpolarization inhibition was abolished 7 min after adding 600 μM-4-aminopyridine (Fig. 7*B*), a dose that reduces the slow-transient potassium current by approximately 50% (Spain *et al.* 1991). Similar results were obtained in four other cells.

Betz cells also possess a fast-inactivating potassium current (Spain *et al.* 1991) but it inactivates within a few milliseconds upon depolarization. This seems too brief to support a reduction of firing rate over hundreds of milliseconds. Nevertheless, we tested whether or not the fast-transient potassium current was involved in post-hyperpolarization inhibition by substitution of cobalt for calcium, a procedure that blocks the fast-transient potassium current (Schwindt, Spain, Foerhing, Stafstrom, Chubb & Crill, 1988*b*). In cobalt the post-hyperpolarization inhibition persisted and voltage clamp (in TTX) revealed that the slow-transient potassium current was present and the fast-transient current was absent in these cells.

After determining the effect of pre-pulses on firing patterns in normal perfusate, the slow-transient potassium current was measured over the range -50 to -30 mV in solutions containing TTX and cadmium, or TTX, 5 mM-$MgCl_2$, 0·5 mM-EGTA and no added calcium. When the slow-transient potassium current was normalized by leakage conductance, no consistent difference in its magnitude was found between cells showing post-hyperpolarization excitation, post-hyperpolarization inhibition or a mixed response. In these experiments, the decline of the slow-transient potassium current over 1 s was measured as a percentage of the peak value during a voltage step

from −70 to −40 mV. Figure 8*B* shows that the decline of the slow-transient potassium current was significantly faster (two-tailed t test, $P < 0{\cdot}05$) in the cells showing post-hyperpolarization inhibition (35 ± 12 %, mean ± S.D., $n = 3$) than in those showing post-hyperpolarization excitation (3 ± 6 %, $n = 3$) or a mixed response (11 ± 11 %, $n = 4$).

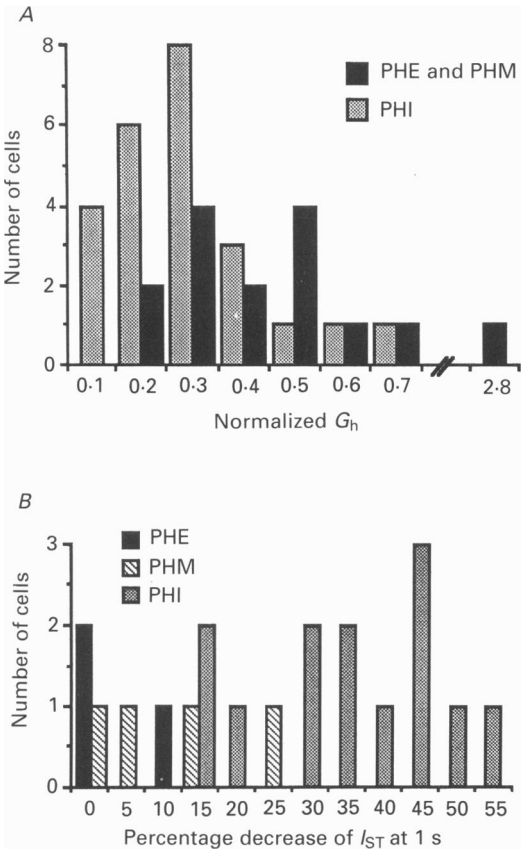

Fig. 8. Differences in G_h and the slow-transient potassium current among cell types. *A*, distribution of the normalized G_h at ≈ −84 mV for cells showing post-hyperpolarization inhibition (PHI) and pooled cells showing either post-hyperpolarization excitation or mixed response (PHE and PHM). Bin width: 0·1. *B*, distribution of the percentage decrease of the slow-transient potassium current (I_{ST}) during a 1 s voltage step from −70 to −40 mV in the three classes of cells. Solution contained TTX and cadmium or TTX, 5 mM-$MgCl_2$, 0·5 mM-EGTA and no added calcium. Bin width: 5 %.

DISCUSSION

In large layer V pyramidal neurones, the firing pattern evoked by a constant current pulse depends on the preceding value of membrane potential. Three distinct responses to pre-pulses were evident. As the pre-pulses were made more negative, the initial firing rate evoked by the test pulse either increased, decreased or did both in sequence during the test current pulse. Other electrical parameters varied with

response type. Cells showing post-hyperpolarization excitation or a mixed response had shorter spike durations and were larger than cells showing post-hyperpolarization inhibition based upon input resistance and anatomical measurements of intracellularly stained neurones. Cells showing either post-hyperpolarization excitation or a mixed response had morphological features similar to cells identified *in vivo* as fast-conducting corticofugal neurones; cells showing post-hyperpolarization inhibition had features of slowly conducting corticofugal neurones. The fast-conducting corticofugal cells have prominent oblique tap root dendrites and both larger somata and less spines on apical dendrites than slowly conducting cells (Deschênes, Labelle & Landry, 1979; Hamada, Sakai & Kubota, 1981; Samejima *et al.* 1985; Yamamoto, Samijima & Oka, 1987).

Several properties of these pyramidal neurones from the cat differ from those of the rat. It is likely, however, that different populations of pyramidal neurones have been studied. Area 4γ of the cat is rich in very large pyramidal neurones (Biedenbach, DeVito & Brown, 1986), but these large cells are absent in rat neocortex (Landry, Wilson & Kitai, 1984). The use of low-resistance microelectrodes in our study restricted our sampling to only the largest neurones. We found that identified large pyramidal neurones in the cat may or may not exhibit adaptation, depending on the preceding membrane potential. In rat neocortex (McCormick, Connors, Lighthall & Prince, 1985) the lack of spike frequency adaptation was associated with identified interneurones. In addition, the briefest spikes occur only in the non-adapting interneurones in the rat neocortex, whereas the largest pyramidal cells in the cat have spikes of comparable duration. Chagnac-Amitai, Agmon & Prince (1988) found that a steady injected current evoked burst firing in the largest pyramidal neurones in layer V_B of rat neocortex. We saw an initial burst in only one cell in this study, and firing rate during the burst was decreased by a hyperpolarizing pre-pulse.

Functional significance

Cheney & Fetz (1980) found that corticomotoneuronal cells of monkey cortex consistently displayed one of four different firing patterns during constant force generation. These response patterns were assumed to result from different temporal patterns of synaptic input. We have found, however, that firing patterns quite similar to those seen by Cheney & Fetz can be evoked in Betz cells by a constant current pulse, depending on the cell type and the preceding membrane potential. In most of Cheney and Fetz's cells (their *phasic-tonic* cells) the high initial firing rate at the onset of force generation declined to a tonic level. That is, firing rate adapted, as was true for most cells in this study when depolarized from resting potential by a constant current pulse. Their *tonic* cells showed little or no adaptation during force generation. We evoked purely tonic firing in cells showing post-hyperpolarization excitation by preceding the test current pulse by a depolarizing pre-pulse. The response of their *phasic-ramp* cells was similar to the cells showing a post-hyperpolarizing mixed response in our study. The response of their *ramp* cells was similar to cells showing post-hyperpolarization inhibition in our study. The various firing patterns in our study resulted solely from the effects of membrane potential on voltage-gated ionic currents. Our results suggest that the membrane properties of individual Betz cells may be as important as neural circuity in shaping firing patterns.

Similar alterations in firing patterns may be produced by neuromodulators in Betz cells. For example, the reduction of calcium- and sodium-mediated potassium currents by noradrenaline or low doses of muscarine abolish slow adaptation, resulting in a more tonic response to a 1 s current pulse (Schwindt, Spain, Foerhing, Chubb & Crill, 1988*a*; Foehring, Schwindt & Crill, 1989). Doses of muscarine > 10 μM cause the firing rate to accelerate to a tonic level during 1 s current pulses (Schwindt *et al.* 1988*a*). However, both noradrenaline and muscarine also increase the final tonic firing rate, whereas conditioning pre-pulses affect only the transient portion of the response. In addition, the conditioning pre-pulses are less influential when the tonic firing is fast, whereas the chemical modulators are more effective at fast firing rates (Foehring *et al.* 1989).

The greatest effects of membrane potential on firing patterns require large, long-lasting hyperpolarizations which must be provided by IPSPs or after-hyperpolarizations in the intact animal. Evoked IPSPs can bring membrane potential to about -75 mV for up to 1 s in layer V pyramidal neurones (Avoli, 1986). Summation of slow after-hyperpolarizations in Betz cells *in vitro* can hyperpolarize the neurones to about -80 mV (Schwindt *et al.* 1988*a*). Prolonged subthreshold membrane potential excursions of at least 10 mV have been recorded from neurones in motor cortex of lightly anesthetized monkeys (Matsumura, Cope & Fetz, 1988). These hyperpolarizations could act as conditioning pre-pulses for any subsequent suprathreshold depolarization, and a hyperpolarization of only 10 mV can cause a threefold increase in peak firing rate of a cell showing post-hyperpolarization excitation (Fig. 2). The recent study of Lemon & Mantel (1989) on cortico-motoneuronal neurones in the monkey suggests that a threefold change in instantaneous firing rate can have a significant effect on motor output.

Mechanisms underlying firing rate modulation

Several of our findings point to I_h activation as the cause of post-hyperpolarization excitation. The time and voltage dependence of both post-hyperpolarization excitation and I_h activation are similar. During depolarization, I_h deactivates with nearly the same time course as the duration of increased firing in cells showing post-hyperpolarization excitation (Spain *et al.* 1987). Caesium causes voltage-dependent reductions both of I_h and post-hyperpolarization excitation that are quantitatively similar. High-frequency firing following a conditioning pre-pulse is not caused by an activation of a low-threshold calcium current because blocking calcium influx has no effect on post-hyperpolarization excitation.

We found that conditioning pre-pulses positive to resting potential cause the initial firing rate to decrease during a test current pulse. Because I_h is small at these conditioning potentials, mechanisms in addition to I_h deactivation must be responsible for the slowed initial firing rates. Voltage steps positive to -60 mV activate a persistent sodium current with fast kinetic properties (Stafstrom, Schwindt, Chubb & Crill, 1985), and the resulting sodium influx activates a potassium current (Schwindt, Spain & Crill, 1989). Activation of this sodium-dependent potassium current could explain the decrease of the initial firing rate observed after depolarizing pre-pulses.

Both post-hyperpolarization inhibition and the two transient potassium currents described in the preceding paper (Spain *et al.* 1991) have similar voltage dependence.

The period of reduced firing, however, corresponded only to the slow inactivation kinetics of the slow-transient potassium current. Additionally, 4-aminopyridine, which selectively reduces the slow-transient potassium current, decreased post-hyperpolarization inhibition, whereas blockade of the fast-transient current with cobalt had no effect. Spikes are so brief that they would have little effect on inactivation of the slow-transient potassium current over many interspike intervals. We conclude that, in cells showing post-hyperpolarization inhibition, it is the removal of partial inactivation of the slow-transient potassium current by the conditioning pre-pulse that causes slowing of firing during a subsequent depolarization.

In cells showing a post-hyperpolarization mixed response that were subsequently subject to voltage clamp, a conditioning hyperpolarization caused the initial membrane current during the test depolarization to become more inward and the late membrane current to become more outward. These results imply that the post-hyperpolarization mixed response is caused by a simple combination of the mechanisms underlying post-hyperpolarization excitation and inhibition. That is, I_h deactivation causes the early period of firing rate increase, whereas increased activation of the slow-transient potassium current causes the late decrease of firing.

The precise role of the slow-transient potassium current is not explained completely by our findings. For example, the slow-transient potassium current is present in cells showing post-hyperpolarization excitation, but there is no evidence that this current was significantly enhanced by hyperpolarizing pre-pulses in either voltage clamp or current clamp. Such an enhancement is expected to cause the late firing rate to decline below the tonic rate after I_h deactivation is complete, as occurs in cells showing the mixed response. Furthermore, the selective reduction of I_h by caesium did not convert the post-hyperpolarization excitatory response to an inhibitory or a mixed response.

A possible clue to this dilemma is the more rapid inactivation of the slow-transient potassium current in cells showing post-hyperpolarization inhibition. The work of others has revealed that macroscopic potassium currents may flow through multiple channel types (e.g. Hoshi & Aldrich, 1988). A recent study of potassium channels cloned from rat brain showed four distinct channels based on voltage dependence and kinetics (Stuhmer, Ruppersberg, Schroter, Sakmann, Stocker, Giese, Perschke, Baumann & Pongs, 1989). We propose that the slow-transient potassium current results from the opening of at least two channel types, an inactivating type and a non-activating type. Some support for this idea is provided by the observation that 4-aminopyridine may preferentially block a slowly inactivating component of the slow-transient potassium current (Spain *et al.* 1991). According to this proposal, the slow-transient potassium current decays rapidly in cells showing post-hyperpolarization inhibition because they contain mostly the inactivating channel type. Consequently, a hyperpolarizing pre-pulse is effective in removing inactivation. Conversely, cells showing post-hyperpolarization excitation exhibit less decay of their slow-transient current because these cells contain mostly the non-inactivating channel type. A hyperpolarizing pre-pulse has little effect on the slow-transient current of these cells because there is little inactivation to be removed. Future studies will attempt to test this hypothesis in identified cell types.

We thank Dr Felix Viana for advice on HRP injection techniques; Lorraine Gibbs for the processing of histological material; Dr Kate Mulligan for guidance in the interpretation of the morphological data; and Todd Cunnington and Sue Blaylock for assistance with manuscript preparation. As usual, Gregg Hinz provided superb technical support. This work was funded by NIH grants NS01166 (W.J.S.), NS16792 and MS20482 (W.E.C. and P.C.S.).

REFERENCES

ADAMS, J. (1981). Heavy metal intensification of DAB-based HRP reaction product. *Journal of Histochemistry and Cytochemistry* **29**, 775.

AVOLI, M. (1986). Inhibitory potentials in neurons of the deep layers of the in vitro neocortical slice. *Brain Research* **370**, 165–170.

BARGAS, J., GALARRAGA, E. & ACEVES, J. (1989). An early outward conductance modulates the firing latency and frequency of neostriatal neurons of the rat brain. *Experimental Brain Research* **75**, 146–156.

BIEDENBACH, M. A., DEVITO, J. L. & BROWN, A. C. (1986). Pyramidal tract of the cat: soma distribution and morphology. *Experimental Brain Research* **61**, 303–310.

CHAGNAC-AMITAI, Y., AGMON, A. & PRINCE, D. A. (1988). Anatomical and physiological properties of bursting cells in layer V_B of somatosensory cortex. *Society for Neuroscience Abstracts* **14**, 883.

CHENEY, P. D. & FETZ, E. E. (1980). Functional classes of primate corticomotoneuronal cells and their relation to active force. *Journal of Neurophysiology* **44**, 773–791.

CONNOR, J. A. & STEVENS, C. F. (1971). Prediction of repetitive firing behaviour from voltage-clamp data on an isolated neurone soma. *Journal of Physiology* **213**, 31–53.

DEKIN, M. S., GETTING, P. A. & JOHNSON, S. M. (1987). In vitro characterization of neurons in the ventral part of nucleus tractus solitarius. I. Identification of neuronal types and repetitive firing properties. *Journal of Neurophysiology* **58**, 195–214.

DESCHÊNES, M., LABELLE, A. & LANDRY, P. (1979). Morphological characterization of slow and fast pyramidal tract cells in the cat. *Brain Research* **178**, 251–274.

EVARTS, E. V. (1968). Relation of pyramidal tract activity to force exerted during voluntary movement. *Journal of Neurophysiology* **31**, 14–27.

FOEHRING, R. C., SCHWINDT, P. C. & CRILL, W. E. (1989). Norepinephrine selectively reduces slow calcium- and sodium-mediated potassium currents in cat neocortical neurons. *Journal of Neurophysiology* **61**, 245–256.

FRIEDMAN, A. & GUTNICK, M. J. (1987). Low-threshold calcium electrogenesis in neocortical neurons. *Neuroscience Letters* **81**, 117–122.

HAMADA, I., SAKAI, M. & KUBOTA, K. (1981). Morphological differences between fast and slow pyramidal tract neurones in the monkey motor cortex as revealed by intracellular injection of horseradish peroxidase by pressure. *Neuroscience Letters* **22**, 233–238.

HORIKAWA, K. & ARMSTRONG, W. E. (1988). A versatile means of intracellular labeling: injection of biocytin and its detection with avidin conjugates. *Journal of Neuroscience Methods* **25**, 1–11.

HOSHI, T. & ALDRICH, R. W. (1988). Voltage-dependent K^+ currents and underlying single K^+ channels in pheochromocytoma cells. *Journal of General Physiology* **91**, 73–106.

LANDRY, P., WILSON, C. J. & KITAI, S. T. (1984). Morphological and electrophysiological characteristics of pyramidal tract neurons in the rat. *Experimental Brain Research* **57**, 177–190.

LEMON, R. N. & MANTEL, G. W. H. (1989). The influence of changes in discharge frequency of corticospinal neurones on hand muscles in the monkey. *Journal of Physiology* **413**, 351–378.

LLINÁS, R. (1988). The intrinsic electrophysiological properties of mammalian neurons: insights into central nervous system function. *Science* **242**, 1654–1666.

LLINÁS, R. & JAHNSEN, H. (1982). Electrophysiology of mammalian thalamic neurones *in vitro*. *Nature* **297**, 406–408.

LLINÁS, R. & YAROM, Y. (1981). Electrophysiology of mammalian inferior olivary neurones *in vitro*. Different types of voltage-dependent ionic conductances. *Journal of Physiology* **315**, 549–567.

MCCORMICK, D. A., CONNORS, B. W., LIGHTHALL, J. W. & PRINCE, D. A. (1985). Comparative electrophysiology of pyramidal and sparsely spiny stellate neurons of the neocortex. *Journal of Neurophysiology* **54**, 782–805.

MATSUMURA, M., COPE, T. & FETZ, E. E. (1988). Sustained excitatory synaptic input to motor cortex neurons in awake animals revealed by intracellular recording of membrane potentials. *Experimental Brain Research* **70**, 463–469.

SAMEJIMA, A., YAMAMOTO, T., ITO, J. & OKA, H. (1985). Two groups of corticofugal neurons identified with pontine stimulation in the cat parietal association cortex: an intracellular HRP study. *Brain Research* **347**, 117–120.

SCHWINDT, P. C., SPAIN, W. J. & CRILL, W. E. (1989). Long-lasting reduction of excitability by a sodium-dependent potassium current in cat neocortical neurons. *Journal of Neurophysiology* **61**, 233–244.

SCHWINDT, P. C., SPAIN, W. J., FOEHRING, R. C., CHUBB, M. C. & CRILL, W. E. (1988*a*). Slow conductances in neurons from cat sensorimotor cortex in vitro and their role in slow excitability changes. *Journal of Neurophysiology* **59**, 450–467.

SCHWINDT, P. C., SPAIN, W. J., FOEHRING, R. C., STAFSTROM, C. E., CHUBB, M. C. & CRILL, W. E. (1988*b*). Multiple potassium conductances and their functions in neurons from cat sensorimotor cortex in vitro. *Journal of Neurophysiology* **59**, 424–449.

SEGAL, M. (1985). A potent transient outward current regulates excitability of dorsal raphe neurons. *Brain Research* **359**, 347–350.

SPAIN, W. J., SCHWINDT, P. C. & CRILL, W. E. (1987). Anomalous rectification in neurons from cat sensorimotor cortex in vitro. *Journal of Neurophysiology* **57**, 1555–1576.

SPAIN, W. J., SCHWINDT, P. C. & CRILL, W. E. (1991). Two transient potassium currents in layer V pyramidal neurones from cat sensorimotor cortex. *Journal of Physiology* **434**, 591–607.

STAFSTROM, C. E., SCHWINDT, P. C., CHUBB, M. C. & CRILL, W. E. (1985). Properties of persistent sodium conductance and calcium conductance of layer V neurons from cat sensorimotor cortex in vitro. *Journal of Neurophysiology* **53**, 153–170.

STAFSTROM, C. E., SCHWINDT, P. C. & CRILL, W. E. (1984). Repetitive firing in layer V neurons from cat neocortex in vitro. *Journal of Neurophysiology* **52**, 264–289.

STORM, J. F. (1988). Temporal integration by a slowly inactivating K^+ current in hippocampal neurons. *Nature* **336**, 379–381.

STUHMER, W., RUPPERSBERG, J. P., SCHROTER, K. H., SAKMANN, B., STOCKER, M., GIESE, K. P., PERSCHKE, A., BAUMANN, A. & PONGS, O. (1989). Molecular basis of a functional diversity of voltage-gated potassium channels in mammalian brain. *EMBO Journal* **8**, 3225–3244.

SUTOR, B. & ZIELGLGÄNSBERGER, W. (1987). A low-voltage activated, transient calcium current is responsible for the time-dependent depolarizing inward rectification of rat neocortical neurons in vitro. *Pflügers Archiv* **410**, 102–111.

YAMAMOTO, T., SAMEJIMA, A. & OKA, H. (1987). Morphology of layer V pyramidal neurons in the cat somatosensory cortex: an intracellular HRP study. *Brain Research* **437**, 369–374.